

## The Fast and Furious in JWST high- $z$ galaxies

MAURICE H.P.M. VAN PUTTEN<sup>1,2</sup>

<sup>1</sup>*Physics and Astronomy, Sejong University  
209 Neungdong-ro, Seoul, South Korea*

<sup>2</sup>*INAF-OAS Bologna, via P. Gobetti, 101, I-40129 Bologna, Italy*

### ABSTRACT

Recent JWST surveys reveal a striking abundance of massive galaxies at cosmic dawn, earlier than predicted by  $\Lambda$ CDM. The implied speed-up in galaxy formation by gravitational collapse is reminiscent of short-period galaxy dynamics described by the baryonic Tully-Fisher relation. This may originate in weak gravitation tracking the de Sitter scale of acceleration  $a_{dS} = cH$ , where  $c$  is the velocity of light and  $H(z) \propto (1+z)^{3/2}$  is the Hubble parameter with redshift  $z$ . With no free parameters, this produces a speed-up in early galaxy formation by an order of magnitude with essentially no change in initial galaxy mass function. It predicts a deceleration parameter  $q_0 = 1 - (2\pi/GAa_{dS})^2 = -0.98 \pm 0.5$ , where  $G$  is Newton's constant and  $A = (47 \pm 6)M_{\odot} (\text{km/s})^{-4}$  is the baryonic Tully-Fisher coefficient (McGaugh 2012). At  $3\sigma$  significance, it identifies dynamical dark energy alleviating  $H_0$ -tension when combined with independent  $q_0$  estimates in the Local Distance Ladder. Conclusive determination of  $q_0 = d \log(\theta(z)H(z))/dz|_{z=0}$  is expected from BAO angle  $\theta(z)$  observations by the recently launched *Euclid* mission.

*Keywords:* JWST — Tully-Fisher — Galaxy formation — Cosmological parameters

### 1. INTRODUCTION

Recent JWST surveys (Eisenstein et al. 2023; Austin et al. 2023) reveal an abundance of massive galaxies in the Early Universe. Extending previous HST high-redshift galaxy surveys (Coe et al. 2013; Oesch et al. 2016) This early galaxy formation faster than expected poses a radically new challenge to  $\Lambda$ CDM (Eisenstein et al. 2005; Boylan et al. 2023; Melia 2023) in addition to the  $H_0$ -tension problem between the Local Distance Ladder and the Planck  $\Lambda$ CDM analysis of the *Cosmic Microwave Background* (CMB) seen in the recent history of cosmological expansion (Aghanim et al. 2020; Riess et al. 2022).

Galaxies form by gravitational collapse of relic density perturbations at the time of the surface of last scattering (Eggen et al. 1962; Gunn et al. 1972; Gott et al. 1975, 1977), marking large-scale structure at the angular scale of *Baryon Acoustic Oscillations* (BAO) in the CMB (Boylan

et al. 2023; Melia 2023; Padmanabhan & Loeb 2023; Gupta 2023). Early galaxy formation by fast collapse is reminiscent of short-period orbital motion in spiral galaxies described by the Tully-Fisher luminosity-velocity relation (Tully&Fisher 1977). Alternative interpretations of the latter by dark matter de Swart et al. (2017); Wechsler & Tinker (2018) and non-Newtonian physics (Milgrom 1983) appear viable but breaking the degeneracy between the two is challenging (Famaey & McGaugh 2012; McGaugh 2012).

A common origin to early galaxy formation and the baryonic Tully-Fisher relation points to non-Newtonian dynamics in weak gravitation *even when applied to dark and baryonic matter combined*. This appears inevitable in the face of the essentially matter-dominated evolution in the early Universe satisfying  $\Omega_M \simeq 1$ , defined by the ratio of total matter density over closure density  $\rho_c = 3H^2/8\pi G$  with Hubble parameter  $H$  and Newton's constant  $G$ .

Generally, galaxy dynamics is mostly in weak gravitation below the de Sitter scale of acceleration  $a_{dS} = cH$ , defined by the Hubble parameter  $H$  and the velocity of light  $c$ . Weak gravitation beyond  $\Lambda$ CDM may be tracking  $a_{dS}$  with observational consequences by redshift dependence (van Putten 2017).

First, it predicts a non-smooth transition to non-Newtonian acceleration. Circular orbits in spiral galaxies can be described by  $a_N/\alpha$  of expected Newtonian acceleration  $a_N$  to the observed centripetal acceleration  $\alpha$  as a function of  $\zeta = a_N/a_{dS}$ . These have a  $C^0$ -transition at  $\zeta = 1$ , observed in a  $6\sigma$  gap between data from the *Spitzer Photometry and Accurate Rotation Curves* (SPARC) and  $\Lambda$ CDM galaxy models (van Putten 2018).

This  $C^0$ -transition can be attributed to a change in the binding energy in the gravitational field of centripetal acceleration  $\alpha$  by the equivalence principle. In the Newtonian limit, the inertia of this binding energy equals a particle's rest mass. This is cut short when accelerations drop below  $a_{dS}$  ( $\zeta$  drops below unity), as the Rindler horizon at  $\xi = c^2/\alpha$  drops beyond the Hubble radius  $R_H = c/H$  (van Putten 2017). This cut gives a  $C^0$ -transition at  $\zeta = 1$  with corresponding radius

$$r_t = \sqrt{R_H R_G} \simeq 4.7 \text{ kpc } M_{11}^{1/2} \propto (1+z)^{-3/4} \quad (1)$$

in galaxies of mass  $M = 10^{11} M_{11} M_\odot$  with gravitational radius  $R_G = GM/c^2$ . Accordingly, high- $z$  galaxies are increasingly non-Newtonian.

The asymptotic regime  $\zeta \ll 1$  of dynamics in disks of spiral galaxies satisfies the baryonic Tully-Fisher relation of total mass  $M_b$  in gas and stars and rotation velocities  $V_c$ , satisfying (McGaugh 2012)

$$M_b = AV_c^4 \quad (2)$$

with  $A \simeq (47 \pm 6) M_\odot (\text{km/s})^{-4}$ . In the absence of dark matter, (2) is described by centripetal accelerations  $\alpha = V_c^2/r$  at radius  $r$ , that can be modeled in terms of a logarithmic potential. Specifically, (2) is equivalent to Milgrom's law  $\alpha = \sqrt{a_0 a_N}$  for short-period orbital motion beyond the Newtonian orbits at  $a_N = GM_b/r^2$ , parameterized by  $a_0 = 1/GA \simeq (1.6 \pm 0.2) 10^{-10}/\text{s}^2$  (Milgrom 1983; McGaugh 2012). However, redshift dependence in  $A(z)$  is inconclusive. High-resolution observations are limited to galaxies at essentially zero redshift (Lelli et al. 2019) and recent observers out to moderate redshifts (Genzel et al. 2017) measure rotation curves limited to moderate radii, intermediate between the asymptotic acceleration  $1/r$  in Milgrom's law and Newtonian acceleration  $1/r^2$  (van Putten 2018).

Second, weak gravitation  $r \gg r_t$  tracking  $a_{dS}$  in (1) predicts redshift dependence in the Milgrom parameter (Fig. 1)

$$a_0(z) = \frac{\sqrt{1 - q(z)}}{2\pi} a_{dS}(z) \propto (1 + z)^{3/2} \quad (z \gg 1), \quad (3)$$

where  $q(z) = -1 + (1 + z)H^{-1}H'(z)$  is the deceleration parameter in a three-flat Friedmann universe.

Here, we show that (3) produces fast galaxy formation at cosmic dawn, explaining the JWST observations with no free parameters. Matter-dominated cosmological evolution covers an extended epoch up down to intermediate redshifts before the onset of the presently observed accelerated expansion (Riess et al. 1998; Perlmutter et al. 1999; Aghanim et al. 2020). This epoch includes primeval galaxy and structure formation since the surface of last scattering ( $z \simeq 1100$ ) when cosmological evolution is described by a Friedmann scale factor  $a(t) \propto t^{2/3}$ ,  $a = 1/(1 + z)$  as a function of cosmic time  $t$ .

In §2, we discuss fast gravitational collapse in weak gravitation defined by  $a_{dS}$ . The consequences for accelerated galaxy formation are quantified in §3. In §4, we summarize our findings with a new estimate of  $q_0$  in tension with  $\Lambda$ CDM.

## 2. FAST GRAVITATIONAL COLLAPSE

Critical to galaxy formation is the time scale of gravitational collapse and the time scale of formation of the first stars and dynamical relaxation. Expansion in the early universe might encompass more time as a function of redshift (Gupta 2023; Melia 2023). This can be modeled by a stretched time  $\tau$ . For instance, power law  $a \propto \tau^n$  gives additional time over  $\Lambda$ CDM by a factor

$$\frac{\tau(z)}{t(z)} = (1 + z)^{\frac{3n-2}{2n}} = \sqrt{1 + n}, \quad (4)$$

where the right-hand side exemplifies linear expansion ( $n = 1$ ) (Melia 2023).

For the ultra-high redshift JWST galaxies,  $\sqrt{1 + z} \sim 4$  appears to be sufficient to satisfy observational constraints on the initial formation rate of the first stars and galaxies (Melia 2023). However, precision cosmology at low redshifts including the ages of the oldest stars in globular clusters are pose stringent constraints on alternative cosmological models. In particular, a cosmology  $a(t) \propto t$ , has a deceleration parameter  $q_0 = 0$ , which is securely ruled out by data of the Local Distance Ladder and Planck  $\Lambda$ CDM analysis of the CMB (e.g. Abchouyeh & van Putten 2021).

Nevertheless, (4) for  $n = 1$  sets a scale for the required speed-up in galaxy formation soon after the Big Bang to accommodate the recent JWST observations. A gain similar to (4) obtains equivalently from dynamical time scales that are sufficiently short, i.e., gravitational collapse times faster than expected from  $\Lambda$ CDM.

Gravitational collapse takes place on a free-fall time scale. Representative analytic expressions are obtained in the two-body problem of radial motion of a test particle to a central mass  $M$  at initial separation  $R_0$  with zero initial momentum. For Newton's force law  $1/r^2$  and  $1/r$  in the baryonic Tully-Fisher relation (2), the respective free-fall time scales are  $t_{ff}^{(2)} = \pi 2^{-3/2} (R_0/a_{N,0})^{1/2} \propto R_0^{3/2}$  and  $\tau_{ff}^{(2)} = \sqrt{\pi} 2^{-1/4} (R_0/\sqrt{a_0 a_{N,0}})^{1/2} \propto R_0$ . Distinct from Newton's theory, the second is not scale-free by coupling to  $a_{dS}$ , leading to scaling with initial separation different from Newton's theory which points to relatively short free-fall time scales. While attributed to reduced inertia, this outcome is

equivalently modeled by constant (Newtonian) inertia in a logarithmic potential. The ratio of the free-fall times hereby satisfies

$$\tau_{ff}^{(2)} = \frac{2^{5/4}}{\sqrt{\pi}} \left( \frac{a_{N,0}}{a_0} \right)^{1/4} t_{ff}^{(2)}, \quad (5)$$

explicitly showing faster gravitational collapse in the regime of weak gravitation, when  $a_{N,0} \ll a_{dS}$ .

### 3. ACCELERATED GALAXY FORMATION

We reinterpret (4) in terms of fast gravitational collapse by (5). By Gauss' law, the Newtonian result in (5) permits a direct generalization  $a_{N,0} = GNm/R_0^2$  for an (initially spherically symmetric) system of  $N$  particles of mass  $m$ , the same does not apply to the logarithmic potential. Hence, the time of gravitational collapse (defined by the time to first bounce prior to virialization) is evaluated numerically. In the large  $N$ -limit,  $N$ -body simulations of initially cold clusters show (Fig. 2) the relations  $t_c = 1.64 t_{ff}$  and  $\tau_c = 1.30 t_{ff}$  for the Newtonian and, respectively, logarithmic potential in (3), the later used to model reduced inertia in weak gravity below  $a_{dS}$ . Here,  $t_{ff} = \pi \langle R_0^{3/2} \rangle / 2\sqrt{2N}$  is the free-fall time-scale of an  $N$ -body cluster with mean  $\langle R_0^{3/2} \rangle$  of the initial particle radial positions  $R_0$ . Importantly,  $t_{ff}$  expresses scaling with  $N^{-1/2}$ , inferred from the exact two-body free-fall time  $t_{ff}^{(2)} = (\pi/2) (R_0/2a_{N,0})^{1/2} a_{N,0} = GM/R_0^2$  initial Newtonian acceleration of a test particle by gravitational attraction at initial separation  $R_0$  to a mass  $M$ . This scaling with  $N^{-1/2}$  for both potentials can be attributed to the tight correlation with virtualization time, the latter dominated by diffusion.

On a cosmological background, the  $N$ -body scaling relations (Fig. 2) and (5) show a speed-up in gravitational collapse

$$B = \frac{t_c}{\tau_c} = 0.94 \left( \frac{a_0}{a_{N,0}} \right)^{1/4} = 1.62 \zeta^{-1/4}, \quad (6)$$

where  $\zeta = a_N/a_{dS}$  (van Putten 2018). Here,  $q = 1/2$  holds on the matter-dominated era at cosmic dawn. Specifically, (6) applies to the scale  $l$  of progenitor mass taken from a perturbation in background closure density  $\rho_c$  feeding the formation of a  $M = 10^9 M_9 M_\odot$  galaxy, i.e.:

$$l \simeq \left( \frac{2M}{\rho_{c,0} \sqrt{\eta} \Omega_{M,0}} \right)^{1/3} \frac{1}{1+z} \simeq \left( \frac{l_0}{1+z} \right) M_9^{1/3}, \quad (7)$$

where  $l_0 \simeq 150$  kpc. By  $a_N = GM/l^2 \simeq (4\pi/3)\rho_c l = (1/2)H^2 l$ ,  $\zeta = a_N/a_{dS} = (1/2)\beta$ ,  $\beta = Hl$ . Speed-up in gravitational collapse (6) hereby satisfies

$$B \simeq 25 M_9^{-\frac{1}{12}} (1+z)^{1/8}, \quad (8)$$

where  $\beta_0 = l_0 H_0 / c \simeq 3.6 \times 10^{-5}$  denotes the local Hubble flow across  $l_0$ .

### 4. CONCLUSIONS

In weak gravitation coupled to  $a_{dS}$ , (8) shows collapse times to be considerably shorter than the Newtonian time scales of  $\Lambda$ CDM. Here, this is parameterized with no free parameters by (3). This

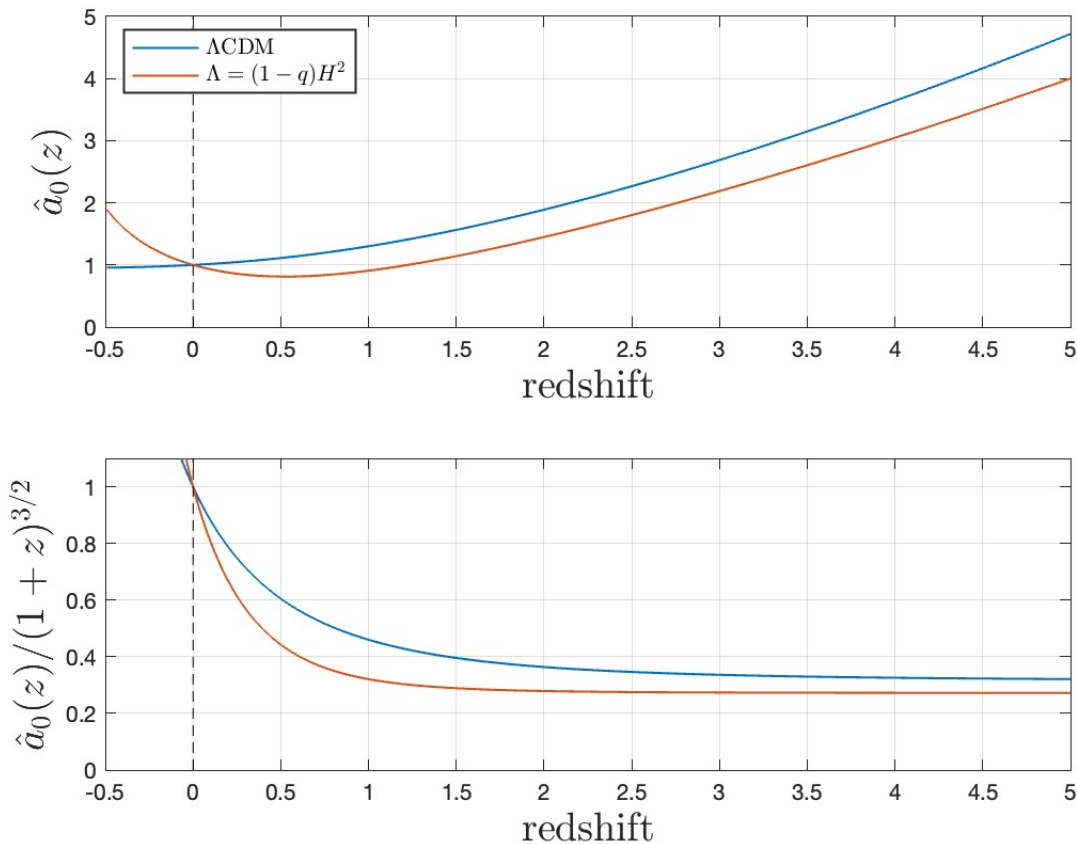


**Figure 1.** Cosmological evolution of  $\hat{a}_0(z) = a_0(z)/a_{0,0}$ , normalized to the present-day value  $a_{0,0} = a_0(0)$ , shown for a background with constant dark energy ( $\Lambda$ CDM) and a dynamical dark energy  $\Lambda = (1-q)H^2$  (the trace of the Schouten tensor) with no  $H_0$ -tension. While  $\hat{a}_0(z)$  increases appreciably in late-time  $\Lambda$ CDM, it varies only slightly in the second.

predicts weak gravitation to govern most of the gravitational interactions in galaxy formation early on identified by JWST. Speed-up (8) in gravitational collapse is over an order of magnitude, sufficient to account for the JWST observations.

With no free parameters, we derive (8) from a natural unification of the baryonic Tully-Fisher relation in late-time cosmology and fast galaxy formation at cosmic dawn. Crucially, (8) is essentially achromatic given a remarkably small power law index  $1/12$  in dependency on galaxy mass, which leaves galaxy mass distributions of  $\Lambda$ CDM effectively unchanged.

The origin of (8) is found in accelerated dynamics beyond the  $C^0$ -transition (1) upon identifying inertia with binding energy in the gravitational field of the accelerating particle (by the equivalence principle). On a cosmological background with a finite Hubble radius  $R_H$ , weak gravitation hereby has a finite sensitivity to  $a_{dS}$ . Expressed by (3), it applies to the asymptotic regime  $\alpha \ll a_{dS}$ , when binding energy (whence inertia) is cut short by the Hubble horizon (van Putten 2017).

For the first time, (3) is confronted at high redshift by JWST observations. The resulting speed-up in galaxy formation (8) takes us closer to cosmic dawn, beyond what can be explained by  $\Lambda$ CDM

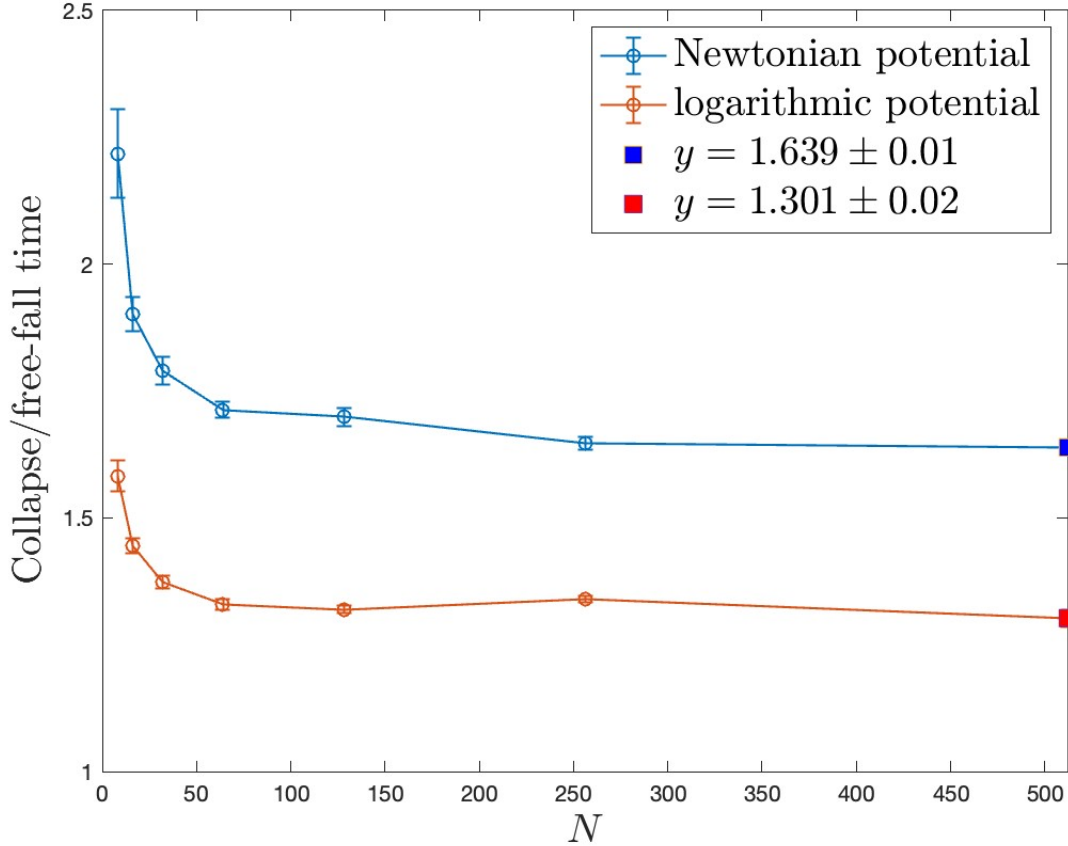


**Figure 2.** The gravitational collapse times of an initially cold system shown for Newtonian and logarithmic potentials by direct numerical simulations with Gaussian initial distributions of  $N$  particles. The logarithmic potential models reduced inertia in the asymptotic regime of weak gravitation tracking  $a_{dS}$ . Both collapse times scale with  $N^{-1/2}$ , here shown by normalization to the Newtonian free-fall time scale  $t_{ff}$ . Generally, collapse times increase by the Hubble flow, more so for the Newtonian than for the logarithmic potential.

galaxy models, in a unification with the baryonic Tully-Fisher relation (2). This confrontation gives clear evidence of galaxy dynamics tracking  $a_{dS}$  (van Putten 2017).

The large speed-up (8) points to the existence of galaxies beyond those currently observed by JWST. These may be detected in upcoming JWST surveys or by ultra-high redshift gamma-ray bursts with the planned *Transient High-Energy Sky and Early Universe Surveyor* (THESEUS) mission (Amati et al. 2018, 2021).

In the more recent epoch of cosmic expansion, (3) expresses sensitivity to the deceleration parameter  $q(z)$  as it drops from matter-dominated ( $q \simeq 1/2$ ) to negative values, signifying accelerated expansion during the present dark energy-dominated epoch. Fundamental to the latter is the combination  $(H, q)$ , parameterized by the present-day values  $(H_0, q_0)$  of the Hubble constant  $H_0$  and deceleration constant  $q_0$ . Inverting (3) gives

$$q_0 = 1 - \left( \frac{2\pi}{GAa_{dS}} \right)^2 = -0.98_{-0.42}^{+0.60} \quad (9)$$

given the baryonic Tully-Fisher coefficient of (20) in (2) and  $H_0 = 73.3 \text{ km s}^{-1} \text{ Mpc}^{-1}$ .

The estimate (9) is consistent with  $q_0 = -1.08 \pm 0.29$  derived from the Local Distance Ladder (Ó Colgain et al. 2019). An even combination of these two independent measurements gives  $q_0 = -1.03 \pm 0.17$  distinct from the Planck  $\Lambda$ CDM value  $q_0 \simeq 0.5275$  (5). At  $3\sigma$  significance, this evidences a dynamical dark energy alleviating  $H_0$ -tension (van Putten 2018,?; Ó Colgain et al. 2019; van Putten 2020)

A decisive result on  $q_0$  - and hence the nature of dark energy - is expected from a survey of the recent expansion history of the Universe by the recently launched *Euclid* mission (35). Specifically, *Euclid* planned measurement of the BAO angle  $\theta(z)$  and  $H(z)$  will provide the radically new measurement

$$q(z) = (1+z) \frac{d}{dz} \log(\theta(z)H(z)). \quad (10)$$

The expected *Euclid* survey of  $\mathcal{O}(10^9)$  galaxies out to a redshift of a few is expected to rigorously distinguish between dynamical dark energy ( $q_0 \simeq -1$ ,  $H'(0) \simeq 0$ ) from  $\Lambda$ CDM ( $q_0 \simeq -0.5$ ,  $H'(0) \simeq H_0$ ) and to reveal the physical nature of low-energy quantum cosmology and the problem of stability of de Sitter space (van Putten 2021).

## 5. ACKNOWLEDGMENTS

We thank M.A. Abchouyeh for stimulating discussions.



## REFERENCES

- Abchouyeh, M. A., & van Putten, M. H. P. M. 2021, PhRvD, 104, 083511
- Planck Collaboration, Aghanim, N., Akrami, Y., 187 et al. 2020, A&A, 641, A6
- Amati, L., O’Brien, P., Gött, D., et al., 2018, AdSpR, 62 191
- Amati, L., O’Brien, P. T., Gtz, D., et al. 2021, ExA, 52, 183
- Austin, D., Adams, N., Conselice, C. J., et al. 2023, ApJL, 952, L7
- Boylan-Kolchin, M. 2023, Nature Astronomy, 7, 731
- Camarena, D., & Valerio, M., 2020, Phys. Rev. Research 2, 013028
- Coe, D., Zitrin, A., Carrasco, M., et al. 2013, ApJ, 762, 32
- Oesch, P. A., Brammer, G., van Dokkum, P. G., et al. 2016, ApJ, 819, 129
- de Swart, J. G., Bertone, G., & van Dongen, J. 2017, Nature Astronomy, 1, 0059
- Eggen, O. J., Lynden-Bell, D., & Sandage, A. R. 1962
- Eisenstein, D. J., Zehavi, I., Hogg, D. W., et al. 2005, ApJ, 633, 560
- Eisenstein, D. J., Willott, C., Alberts, S., et al. 2023, arXiv e-prints, arXiv:2306.02465
- Euclid Mission (ESA), 2023, [https://www.esa.int/Science\\_Exploration/Space\\_Science/Euclid](https://www.esa.int/Science_Exploration/Space_Science/Euclid)
- Famaey, B., & McGaugh, S. S. 2012, Living Reviews in Relativity, 15, 10
- Genzel, R., Förster Schreiber, N. M., Übler, H., et al. 2017, Nature, 543, 397
- Gott, J. R., I. 1977, ARA&A, 15, 235
- Gott, J. R., I., & Rees, M. J. 1975, A&A, 45, 365
- Gunn, J. E., & Gott, J. Richard, I. 1972, ApJ, 176
- Gupta, R. P. 2023, MNRAS, 524, 3385
- McGaugh, S. S. 2012, AJ, 143, 40
- Melia, F. 2023, MNRAS, 521, L85
- Milgrom, M. 1983, ApJ, 270, 365
- Lelli, F., McGaugh, S. S., Schombert, J. M., Desmond, H., & Katz, H. 2019, MNRAS, 484, 171 3267
- Ó Colgáin, É., van Putten, M.H.P.M., & Yavartanoo, H., 2019, Phys. Lett. B, Padmanabhan, H., & Loeb, A. 2023, arXiv:2306.04684
- Perlmutter, S., Aldering, G., Goldhaber, G., et al. 185 1999, ApJ, 517, 565
- Tully, R. B., & Fisher, J. R. 1977, A&A, 54, 661
- Wechsler, R. H., & Tinker, J. L. 2018, ARA&A, 203 56, 435
- Riess, A. G., Filippenko, A. V., Challis, P., et al., 1998, AJ, 116, 1009
- Riess, A. G., Yuan, W., Macri, L. M., et al. 2022, ApJL, 934, L7
- van Putten, M. H. P. M. 2017, ApJ, 848, 28
- van Putten, M.H.P.M., 2018, MNRAS, 481, L26
- van Putten, M.H.P.M., 2021, Physics Letters B, 823, 136737
- van Putten, M.H.P.M., 2018, in ICGAC-XIII and IK-15 on Grav., Astroph. and Cosmology, EPJ Web Conf. 168, 08005; Deriving  $A$  from  $a_0$  from galaxy rotation curves requires care in the extrapolation of a finite range of values  $x = a_N/a_0$ , typically down to  $x = a_N/a_0 = \mathcal{O}(10^{-2})$ . This may incur systematic errors depending on interpolation between  $\zeta \ll 1$  and  $\zeta \geq 1$ . Conventional interpolation  $f(x) = x/(1+x)$  does not take into account the  $C^0$ -transition at  $\zeta = 1$ , producing an underestimate of 20% compared to a more detailed theoretical fit. Corrected for this transition,  $a_0 \simeq 1.6 \times 10^{-8} \text{cm s}^{-1}$  consistent with  $A$  in the baryonic Tully-Fisher relation (2)
- van Putten M.H.P.M., 2020, MNRAS, 491, L6